

A BUILDING ENVELOPE CHARACTERIZATION WORKFLOW FOR IN-SITU THERMAL PERFORMANCE ASSESSMENT

Tyler Pilet* and Tarek Rakha
School of Architecture, Georgia Institute of Technology, Atlanta, GA

*Corresponding Author Email: tpilet@gatech.edu

ABSTRACT

As buildings age, retrofits are becoming an increasingly important topic for the ever-growing and aging existing building stock. With 50% of American buildings built before 1980 and only 0.5–1% of existing buildings retrofitted annually, thermography can be used to non-intrusively characterize building envelopes to inform energy modeling, façade design, and project appraisal for potential projects. This paper presents a short review of literature and published methods to characterize existing building envelopes' thermal properties, followed by a preliminary thermography-based methodology to characterize the thermal resistance and thermal mass properties of a building envelope. The proposed methodology utilizes optimization-enabled transient finite elements to characterize envelope thermal properties. The verification of this methodology showcased that the proposed finite-element workflow can adequately characterize an envelope's thermal performance. This methodology serves as a foundation for future research in building envelope defect characterization.

INTRODUCTION

The US Department of Energy reports that 42% of energy use in buildings is a result of thermal losses through a building's thermal envelope (DOE, 2012; EIA, 2012). While new buildings are typically governed and inspected according to the jurisdiction's building codes, defects can still occur in a building's thermal envelope. Defects result in heat shortcutting the insulation specified within code, rendering diligent insulation practices ineffective. With 50% of the US building stock constructed before 1980 (IEA, 2019) and only 0.5-1% of existing buildings being renovated annually (Architecture 2030, 2018), a non-intrusive method for evaluating the thermal performance of existing building envelopes is required for the building industry.

In the past, much work has been done in the field

of thermography and building assessment to identify defects in the built environment, but the practice has varied little in recent years. Assessors utilize images of thermal anomalies to diagnose faults in buildings façades. Thermal imaging for building inspection acts similarly to a trade where experience is the key to quality work. Anyone with a thermal camera can quickly locate a thermal anomaly, but only the experienced can adequately identify and diagnose anomalies with certainty. This practice has spawned an entire field at the intersection of thermal imaging and building inspections and has made the tool invaluable to the field of building assessment (Balaras & Argiriou, 2002).

While thermal imaging is an informative tool in its own right, it is unable to characterize envelope performance or composition with the technology alone. By leveraging the insights of thermal imaging, thermal modeling can be employed to non-intrusively characterize an envelope's thermal properties and the impacts of deterioration and defects. Once a defect is identified and characterized, this information can be used to identify the origin and severity of identified defects. This computational process is not exclusive to thermal imaging and can be applied with forms of thermal measurement; however, thermal imaging is the most ubiquitous in auditing and easily accessible means of non-intrusively locating defects.

This paper will comprise a survey of relevant thermal characterization research present within the building industry; a proposition of a preliminary methodology and a simulation-based experiment to verify this experiment. The goal of this paper is to provide a foundation for future research in thermal characterization and forensic testing of envelope defects.

EXISTING MODELING TECHNIQUES

There are two main types of engineering models to be considered when evaluating thermal performance: forward models and inverse models. A forward model requires user inputs of physical properties and geometry

into a model or equation to compute a given output for a system. Energy modeling is an example of this, as energy models require significant effort to prescribe inputs and generate geometry to predict energy usage and thermal loads for buildings. Forward models are a frequented area in engineering research; however, forward models cannot predict the performance of a system where model inputs are unknown.

Alongside forward models, another modeling type is the inverse model. As the name suggests, this is the inverse of a forward model. Inverse models take measured inputs of performance and quantify the physical parameters required to produce measured data. Typical inverse models identify model parameters by running a forward model alongside an optimization algorithm to minimize the error between simulated and actual results. A frequented example of inverse modeling is energy model calibration, where optimization algorithms are used to identify model parameters (i.e. occupancy, number of lights, thermostat setpoints, etc.) that minimize the difference of simulation and utility data (Heo, Choudhary, & Augenbroe, 2012). From this viewpoint, thermal characterization is simply a model calibration exercise. Since forward models are a fundamental component in an inverse modeling exercise, the vast body of research in forward thermal modeling can be leveraged to produce inverse models for characterization of building façades. Due to the goals of this work, this paper will focus only on inverse modeling approaches, rather than forward modeling.

REVIEW OF INVERSE MODELING TECHNIQUES

Much like forward models, inverse models are either physics-based or data-driven, with data-driven models becoming increasingly common for inverse modeling (Zhang, O'Neill, Dong, & Augenbroe, 2015). The research in forward modeling can be leveraged with the use of optimization and calibration techniques to repurpose a forward model for the use of inverse modeling (R. Kramer, van Schijndel, & Schellen, 2012).

Lumped Capacitance Inverse models

The lumped capacitance method is a frequented physics-based model used for inverse modeling due to its small computational overhead and simple implementation. This method utilizes an assembly effective thermal resistance, denoted as R , and a “lumped” thermal capacitance value for the entire assembly, denoted as C . Similar to typical forward modeling approaches, there are lumped capacitance inverse models to predict indoor conditions (R. P. Kramer & van Schijndel, 2012) and façade performance (Alshatshati, 2017). Most physics-based models used in

inverse modeling are shaped as 2R1C models, with 3R2C and more complex models falling into the background due to increasing computational overhead. While this method is frequented often in literature, the accuracy drawbacks of the lumped capacitance model make it a less desirable method for characterization (Antonopoulos & Koronaki, 1998).

Finite Element Inverse Models

Finite element models seem to be less frequented in inverse modeling due to their significant computational requirements. This does not entirely stop the method's use, as it was first used in 1978 by Krutz et al. to characterize the thermal properties of a heated rod (Krutz, Schoenhals, & Horc, 1978). Krutz et al. showed that this an inverse finite element method model can predict thermal properties with much success in 1D. This work was followed by Tseng et al. in 1995, who developed a 2D finite element inverse that showed much promise (Tseng, Chen, & Zhao, 1995). Finite element inverse modeling was not directly applied to the building industry until van Schijndel utilized COMSOL to characterize the hygrothermal properties of a façade with marginal accuracy (van Schijndel, 2009). Regardless of the experiment's accuracy, van Schijndel emphasized the importance of their method and potential for future façade characterization applications, i.e. thermography. Since then, thermal characterization of building façades does appear to have been approached with finite elements. The only other relevant application in this time is characterization insulation compression defects with 3D finite elements (Aïssani, Chateaneuf, Fontaine, & Audebert, 2016). While this work is important, such a complicated and expensive method may not be possible when characterizing an entire façade.

Conduction Transfer Function Inverse models

While transfer functions are a widely popular method for thermal modeling, they are not as frequently used in inverse modeling. J.E. Braun used transfer functions to create an inverse model of indoor temperature and characterize building envelopes for many years (Braun & Chaturvedi, 2002), and is one of the only authors to have utilized conduction transfer functions for explicit façade characterization.

Since transport functions are the primary forms of conduction heat transfer calculation in DOE2, BLAST, and EnergyPlus, most calibration and inverse modeling exercises in these energy modeling programs can be reformulated for calibration of façades. This means that the body of research on energy modeling calibration is relevant and can be applied to characterize a building's façade using thermal loads, energy usage, and modeled surface temperatures (Haberl & Bou-Saada, 1998; Heo et al., 2012). Utilization of energy modeling software for

inverse modeling is a convenient way to leverage transfer functions with limited heat transfer knowledge.

Data-Driven Inverse models

There are many types of data-driven models used to characterize building thermal performance. Most of the data-driven models for façades can be classified as grey or black-box models, where models are either supervised or unsupervised in engine calculations.

There are few grey box studies relating to building façade characterization, with one choice being the AutoRegressive-Moving-Average model with eXogenous inputs (ARMAX) algorithm. The first study of this kind is by Norlén, who characterized the thermal envelope of a test cell using the ARMAX algorithm informed by a steady-state thermal model (Norlén, 1990). The most recent study on grey box inverse modeling for buildings is that of Jiménez et al. (Jiménez, Madsen, & Andersen, 2008). This study leverages the data-driven approach of ARMAX alongside lumped capacitance modeling to evaluate the indoor temperature of a test building. If properly trained, this type of model could be utilized rather than a physics-based algorithm for high-speed façade characterization.

Another implementation of data-driven inverse modeling for thermal characterization is neural networks. Neural networks have recently become popular in many fields, but little work has been done with neural networks in thermal characterization. The first study utilizing neural networks for characterization is that of Chen and Chen. This work utilized neural networks to determine the transport functions of a test building's façade with reasonable accuracy (Chen & Chen, 2000). This paper shows that there is a possibility of combining computationally inexpensive transport functions with another technology to quickly and characterize a building's thermal performance.

Besides the work of Chen and Chen, few other applications of neural networks in thermal characterization have been published. Work has been done utilizing neural networks and computer vision to identify defects in thermography; however, none of these works have aimed to characterize envelope thermal performance (Cho, Bianchi-Berthouze, Marquardt, & Julier, 2018; Rakha & Gorodetsky, 2018; Vallerand & Maldague, 2000). While these applications of computer vision and machine learning do not directly address the task of thermal characterization of building envelopes, these works do contribute to characterization efforts. Anomaly detection is a fundamental step for thermal characterization of building envelopes.

While all of the previous data-driven studies utilized measurements and physical properties, databases based upon building age, or building vintage, are widely used for urban modeling. Knowing the year

of a building's construction allows for databases of local energy codes and similar building types to be parsed to characterize the building's façade assembly (Reinhart & Cerezo Davila, 2016). Current urban-scale energy models such as CityBES, CitySIM, SUNtool, UMI, and Virtual EPB all automate urban-scale modeling with the use of CityGML (Reinhart & Cerezo Davila, 2016). While the use of a façade database may not identify the exact properties of a building façade, the use of these databases in assessment may provide an expectation or starting point for characterization methods.

Concluding Remarks

In total, 67 papers were evaluated within this literature review, and specific approaches were used for specific tasks. A scorecard summarizing the subjective performance of each model can be found in Table 1.

Table 1 A tabulated performance summary of reviewed heat transfer modeling techniques.

Model	Speed	Accuracy	Ease of Implementation	Inverse Modeling Potential
Lumped Capacitance ¹	3	2	3	2
Finite Difference ²	2	3	3	2
1D Finite Element ³	3	3	1	3
2D Finite Element ⁴	1	3	1	1
Transfer Function ⁵	3	3	2	3
Data-Driven ⁶	3	2	1	3

Legend: 3–Good, 2–Acceptable, 1–Poor

Sources: ¹(Wang & Xu, 2006), ²(Grossmann, Roos, & Stynes, n.d.), ³(Krutz et al., 1978), ⁴(Tseng et al., 1995), ⁵(Xu & Wang, 2008), ⁶(Alshatshati, 2017)

In this abridged literature survey, a variety of papers with application in different areas and diverse computational approaches were reviewed. While this paper does not present an exhaustive literature review of all thermal modeling literature within the field of building science, it was noted that only a few papers focused on the modeling of defects. All papers focused on defects also approached defect evaluation from a forward modeling approach, leaving a literature gap in inverse modeling of building façade defects. Due to this lack of representation, a literature gap for characterization of defects in façades has been identified and will be the focus of future work. To achieve this goal, previous work in inverse modeling of façades can be leveraged as a starting point to characterize the entire façade, then new methods should be developed to

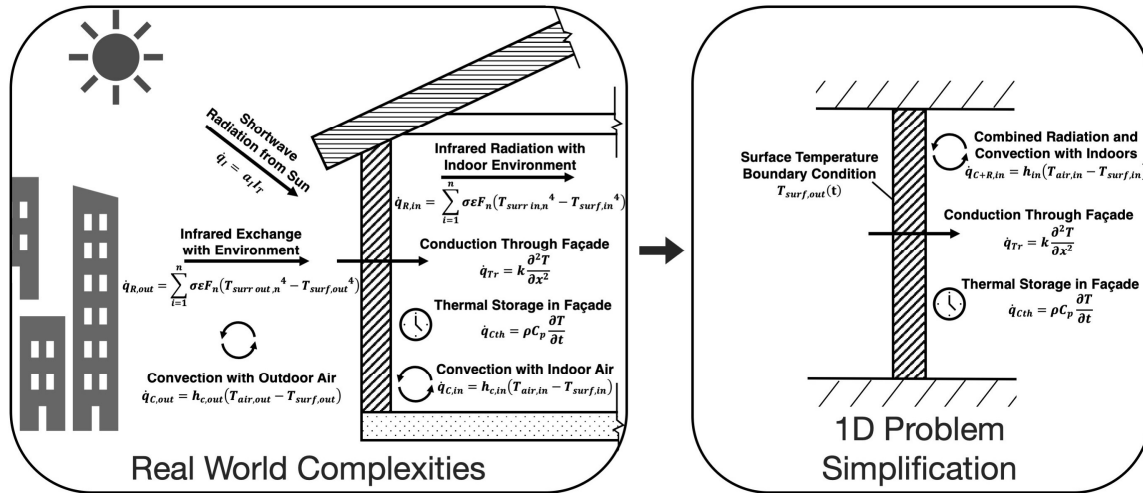


Figure 1 A graphical representation of the heat transfer influencing façade thermal performance, which can be reduced to a simplified system with the use of a surface temperature measurement.

characterize the impact of specific façade defects.

THEORY

To evaluate the potential to characterize a building's façade through thermography, a transient thermal model was developed. This model computes the heat transfer and temperature at surfaces of the building element, allowing for comparison with the measured data. A summary of the modes of heat transfer computed within this model can be seen graphically in Figure 1.

In the figure, a variety of modes of heat transfer are computed. Shortwave radiation, longwave radiation, and convection heat exchange with the outdoor environment are computed for exterior surfaces of the façade, transient conduction is computed for through the façade element, and combined longwave radiation and convection with the indoor environment is computed for the interior surface. Balancing these modes of heat transfer among their respective surfaces can provide the interior and exterior surface temperatures of the façade element, which in turn can be utilized to characterize the thermal properties of the façade element in 1D.

Computing the various modes of heat transfer on the exterior of a façade element is no simple task; numerous environmental and local variables contribute to heat transfer. This complexity motivates the usage of the heat balance approach proposed within ASHRAE Fundamentals (2013 ASHRAE Handbook—Fundamentals, 2013). While it may seem like a monumental task to characterize a façade under all of these time-dependent factors and heat balancing, the task can be drastically simplified with the usage of a surface temperature measurement. Shortwave radiation, environmental longwave radiation, and local convection all contribute to the exterior surface temperature of the façade element, meaning that they can be represented in the exterior surface temperature of the façade. If all

forms of exterior heat transfer are represented as surface temperature, the complexity of the heat balance approach can be avoided and applied as a simple temperature boundary condition in a 1D transient conduction problem. Interior surface heat transfer can also be simplified as a combined longwave-convection heat transfer coefficient since most interior partitions can be assumed to be the temperature of the interior air. This simplification can be seen in the latter half of Figure 1.

Thermal Characterization

In this work, a two-stage characterization process is proposed: The former involves instrumentation of the real building, and the latter stage is an optimization-based inverse heat transfer computation. This approach is summarized graphically in Figure 2. The first stage is an instrumentation and data collection stage conducted over a sufficiently long time frame, with the higher the frequency and longer the time frame being preferable. Once data is collected for a sufficiently long time with an appropriate measurement frequency, the computation stage can be run. This stage utilizes the exterior temperature measurements as a temperature boundary condition within the finite element approach and assumes a convective boundary condition with a fixed convection coefficient on the interior side. The transient conduction is handled via the transient finite element method (FEM) to characterize the thermal equivalent of a layered façade element.

In this approach, material properties such as thermal conductivity, specific heat, and density are treated as thermal resistance and thermal capacitance. These terms can be computed with Eq. 1 and 2.

$$R = \frac{L}{k} \quad (\text{Eq. 1})$$

$$C_{th} = LC_p \rho \quad (\text{Eq. 2})$$

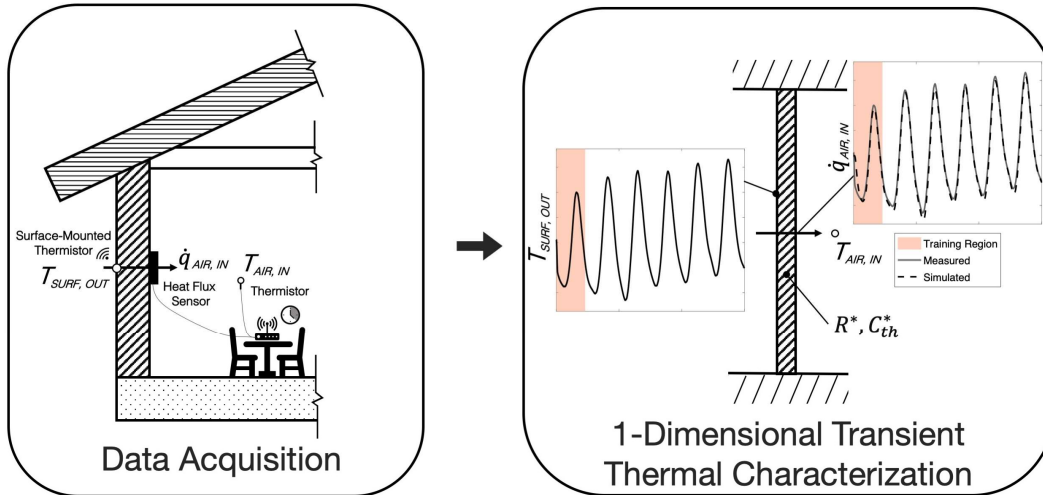


Figure 2 The two proposed stages for in-situ building envelope characterization.

Where R is the thermal resistance of an element, L is the thickness of the element, k is thermal conductivity, C_{th} is the thermal capacitance or thermal mass of the element, C_p is the specific heat, and ρ is density.

With the thermal performance of a façade element is expressed in terms of thermal resistance and thermal capacitance, optimization can be used to determine the representative thermal properties of a façade. This can be accomplished with the optimization statement in Eq. 3, adapted from ASTM C1155 (ASTM, 2013b):

$$\begin{aligned} \text{For each face and} & \sum_{i=1}^n (\dot{q} - \hat{q}(R, C_{th}))^2 & \text{(Eq. 3)} \\ \text{defect, minimize:} & \\ \text{Subject to:} & 0 < R \leq 100 \frac{m^2 \cdot K}{W} \\ & 0 < C_{th} \leq 150,000 \frac{J}{K \cdot m^2} \end{aligned}$$

Where \dot{q} is measured interior surface heat flux, \hat{q} is the simulated interior heat flux, R is the overall thermal resistivity of the façade element, and C_{th} is the total thermal capacitance of the façade element. Eq. 3 allows for the characterization to locate with the same heat transfer as the measured assembly. Typically, the thermal performance of building facades is measured via an exterior surface-mounted temperature sensor and a heat flux sensor mounted on the interior surface of the envelope, motivating the use of heat flux in the objective function. While thermal characterization is typically conducted via a surface mounted sensor, this approach has many drawbacks. Most notably is the American Society for Testing and Materials (ASTM) suggestion to place multiple heat flux sensor-exterior thermistor combinations on multiple test points on a façade element, since “A single [heat flux transducer] site is not representative of a building component. [Use] multiple sensor sites to assess overall performance of a building component (ASTM, 2013a).” The process of placing multiple sensors can be very time and labor-intensive, so

a new method utilizing two thermal cameras is proposed to facilitate the characterization process.

This approach utilizes two thermal cameras in place of the mounted heat flux and temperature sensors to measure surface temperatures at the interior and exterior surfaces of the façade. This approach also allows for the façade to be modeled via 1D finite elements using temperature and convective boundary conditions. The computational workflow of this approach is the same as the one with a heat flux sensor, allowing for the proposed method to be applied to either. Surface temperature can be converted to interior heat flux using a convective boundary condition allowing for assembly characterization with the same objective function as a flux sensor-based instrumentation.

EXPERIMENTAL DESIGN

To evaluate the performance of the inverse modeling procedures proposed above, a sample characterization exercise was applied to a simulated building to mimic a real building assessment without the uncertainties of the real world. The building utilized is a DOE/IECC 2015 medium office reference building simulated with the Hartsfield-Jackson Atlanta TMY3 weather file in EnergyPlus (Deru et al., 2011; DOE, 2020). The simulated building can be seen in Figure 3.

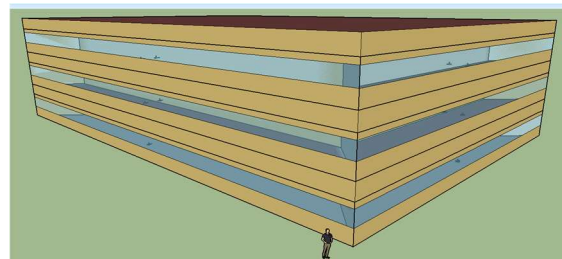


Figure 3 The simulated EnergyPlus model geometry.

To test the characterization workflow, the South-facing wall of the bottom floor will be characterized by both methods. Simulation of this building within EnergyPlus allows for surface temperatures of the interior and exterior and heat fluxes to be measured, simulating instrumentation and data collection on a real building. This measured data is also quite useful for this early-stage testing since it is free of measurement and calibration error present in real-world experimentation.

The simulated building will provide measured interior and exterior surface temperature data for 1–5 January and 1–5 July for summer and winter assessments. The wall constructions of the building will also be varied to test the methodology’s performance on low and high mass walls. The wall constructions utilized in this simulation were taken from the sample nonresidential construction found in ASHRAE Fundamentals Ch. 18 (2013 ASHRAE Handbook—Fundamentals, 2013). A summary of these walls can be seen in Table 2 below.

Table 2 ASHRAE Fundamentals wall assemblies utilized within the building simulation.

Layer Number	Low Mass Wall (Wall #13)	High Mass Wall (Wall #63)
1	25mm Stucco (F07)	200mm Heavyweight Concrete (M15)
2	13mm Fiberboard Sheathing (G03)	89mm Batt Insulation (I04)
3	89mm Batt Insulation (I04)	89mm Batt Insulation (I04)
4	16mm Gypsum Board (G01)	16mm Gypsum Board (G01)

RESULTS

Two differential trials were tested to evaluate model performance on low mass and high mass constructions. Both façade elements were simulated in EnergyPlus for a DOE/IECC 2015 medium office reference building simulated for the climate of Atlanta, Georgia. Models were trained on interior heat flux measurements utilizing the MATLAB surrogate optimization algorithm. Measured heat flux was computed from model output interior wall surface temperatures, interior zone air temperatures, and a constant convection coefficient. Both models also received temperature boundary conditions on the exterior surface of the wall, measured via the EnergyPlus simulation. Both models were trained for 48 hours of data measured at 10-minute intervals, and models were evaluated utilizing 52 hours of measured data occurring after the training period.

Low Mass Wall Thermal Characterization

The first trial was run assessing a south-facing Wall #13 for the first week of January. The results of this study are presented in Figure 4.

Flux-Based 48 Hour Low Mass Wall Characterization

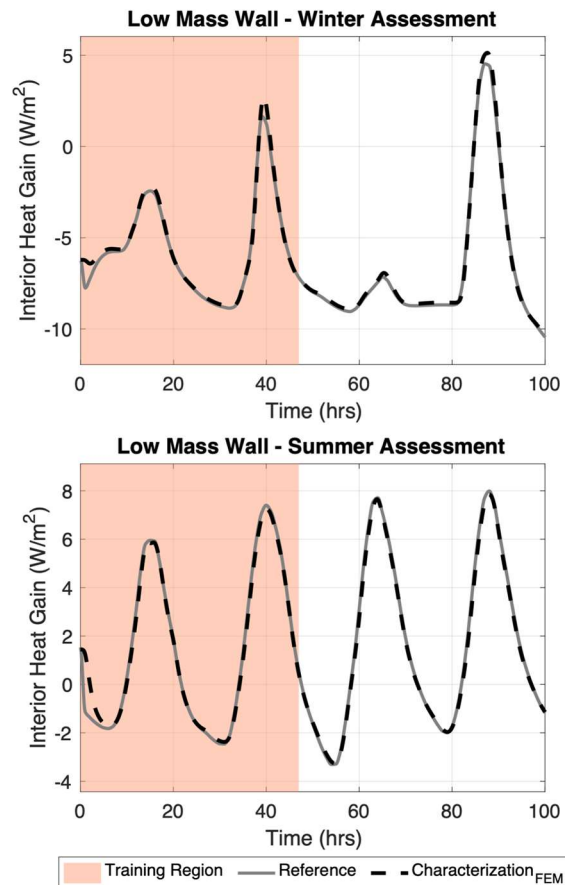


Figure 4 Plotted interior heat gain from a 48-hour characterization of a low mass wall.

From the above figure, the performance of the finite element characterization can be seen. The exercise characterized the façade element with R-Squared values greater than 0.990 for both winter and summer. A summary of the thermal characterization results can be seen in Table 3.

Table 3 Characterization results for a low mass wall.

Test Case	Thermal Resistance, R	Lumped Capacitance, C_{th}	R-Squared Value
Simulated Façade	2.105	61,699	N/A
Winter	2.184	13,918	0.998
Summer	2.294	13,999	0.999

From Table 3, the results of the characterization exercise for the low mass wall can be seen. The characterized single-layer walls for winter and summer had similar thermal resistances to the “real” wall, with percentage errors of 3.755% and 8.979% for winter and summer compared to the simulated wall, respectively.

While thermal resistances were characterized well for both cases thermal capacitance values characterized at 77.414% and 77.323% percentage difference compared to the lumped capacitance of the reference wall, while the modeled heat transfer closely mimics that of the measured wall.

High Mass Wall Thermal Characterization

The second trial was run for Wall #59 utilizing the same spatial and environmental conditions as the previous exercise. The results of this study are presented in Figure 5.

Flux-Based 48 Hour High Mass Wall Characterization

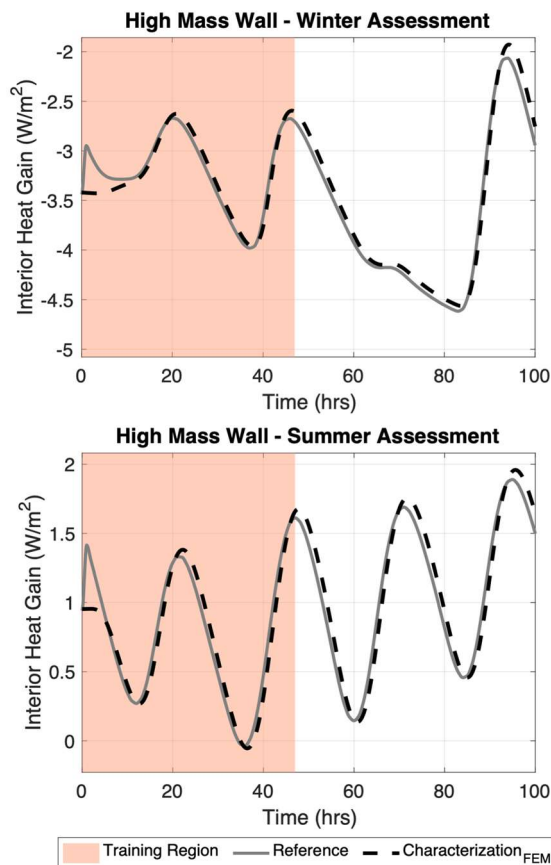


Figure 5 Plotted interior heat gain from a 48-hour heat flux-based characterization for a high mass wall.

A summary of the thermal characterization results can be seen in Table 4.

Table 4 Characterization results for a high mass wall.

Test Case	Thermal Resistance, R	Lumped Capacitance, C_{th}	R-Squared Value
Simulated Façade	4.065	233,978	N/A
Winter	4.214	61,456	0.971
Summer	4.017	66,240	0.955

Table 4, displays the results of high mass wall characterization. The characterized single-layer walls for winter and summer had similar thermal resistances to the “real” wall, with percentage differences of 3.67% and 1.18% for winter and summer, respectively. The relative size of this error and similarity of results for summer and winter tests suggest that the wall’s insulating value was properly characterized through this procedure.

Once again, thermal capacitance values characterized at 73.734% and 71.690% percentage difference from the lumped capacitance of the multi-layered assembly.

DISCUSSION

This study shows the promise of characterizing façades utilizing transient finite element heat transfer. The results for Wall #13 and Wall #59 thermal characterization during summer and winter show good model agreement with measured data, with R-squared values of 0.998 and 0.999 for summer and winter characterizations and R-squared values of 0.971 and 0.955 for summer and winter characterizations of Wall #59. For all four testing cases, thermal resistance was characterized within a 10% error of the resistivity of the measured wall which verifies the characterization of thermal resistance.

While all simulated transient models had good agreement with measured data and thermal resistance was found to be adequately characterized, thermal capacitance was not found to be near the lumped thermal capacitance value of the real multi-layer wall. This occurs because a single lumped capacitance of a multi-layer wall is not an appropriate means to simulate the performance of a complex multi-layer assembly (Antonopoulos & Koronaki, 1998; Ramallo-González, 2013). Instead of expecting the thermal capacitance of a single-layer thermally equivalent wall to match that of a multi-layered wall, thermal resistance should be compared to evaluate characterization performance. Viewing R-squared values of the characterization results show that the characterized single-layer walls adequately mimic the performance of the simulated multi-layer wall. This indicates that the characterization process located a thermally equivalent wall, despite having a different thermal capacitance. This means that a single material,

with its associated thermal resistance and thermal capacitance, appropriately represents the complex interactions between various thermal capacitances and thermal resistances of the multi-layered wall without the need to simulate this complexity. This result also indirectly shows that the thermal mass of each layer in an assembly cannot be simply added up and modeled; a thermally equivalent wall must be found instead.

These results of this study show a large potential for thermal characterization growth in the built environment. Utilizing surface temperatures and heat flux measurements, any type of opaque façade element can be simulated to understand its performance. While this work was able to characterize the thermal performance of a typical façade element, the hope is that this procedure is used more often in the future to understand the impact and origin of defects in building façades. In practice, defects are located via thermal imagery and façade R-values are found, but both processes are separate. Utilizing the workflow presented in this work both processes can be brought together to locate envelope defects and understand their impact simultaneously.

CONCLUSION

This study surveyed literature relevant to forward and inverse thermal modeling in the field of building science. Few studies focused on inverse thermal for façade and defect characterization, so a thermography-driven inverse thermal modeling procedure was proposed and tested with simulation data within this paper. This procedure uses transient finite elements in an optimization-enabled inverse modeling workflow to identify thermally equivalent materials representing the complexity of thermal mass and thermal resistance in multi-layer assemblies. This procedure was successful when tested, characterizing low and high mass walls with R-Squared values all above 0.950.

The robust and proven performance of this characterization process opens the door to understanding more about how building envelopes perform in the real world. This process is also generalizable enough to characterize defects in the built environment, allowing for building owners to truly understand the impact of defects in their home or business. While this work is effective in simulation test cases, the workflow requires field testing for validation in future studies. Applying this method in the real world will also allow for defects to be characterized and understood, which is a reality whole-building simulation packages, like EnergyPlus, fail to reproduce.

This study is a fundamental step in the process of detecting, characterizing, and understanding the impact of defects in existing buildings. Now that the

performance of individual façade components can be characterized, work can be done to further explore the performance of the complex whole-building envelope. This work sets a basis, as it paves the way for future work into the relatively unexplored field of façade defect characterization and modeling.

NOMENCLATURE

Symbol	Name	Unit
Latin Characters		
a_l	Solar Absorptance	Unitless
C_{th}	Thermal Capacitance	$\frac{J}{K - m^2}$
C_p	Specific Heat Capacity	$\frac{J}{kg - K}$
F	View Factor	Unitless
h	Convection Coefficient	$\frac{W}{m^2 - K}$
I	Solar Irradiance	$\frac{W}{m^2}$
k	Thermal Conductivity	$\frac{W}{m - K}$
L	Length	m
R	Thermal Resistance	$\frac{m^2 - K}{W}$
\dot{q}	Heat Flux	$\frac{W}{m^2}$
t	Time	s
T	Temperature	°C, K
Greek Characters		
ϵ	Longwave Emissivity	Coefficient
ρ	Density	$\frac{kg}{m^3}$
σ	Stefan-Boltzmann Constant	Coefficient
Subscripts		
<i>air</i>	Ambient Air	
<i>C</i>	Total Convection	
<i>C_{th}</i>	Thermal Mass Storage	
<i>in</i>	Indoor	
<i>out</i>	Outdoor	
<i>surf</i>	Surface	
<i>surr</i>	Surrounding Context	
<i>T</i>	Total	
<i>Tr</i>	Conduction Transmission	

REFERENCES

- 2013 ASHRAE Handbook—Fundamentals. (2013). Retrieved from <https://www.ashrae.org/technical-resources/ashrae-handbook>
- Aïssani, A., Chateaufneuf, A., Fontaine, J. P., & Audebert, P. (2016). Quantification of workmanship insulation defects and their impact on the thermal performance of building facades. *Applied Energy*. <https://doi.org/10.1016/j.apenergy.2015.12.040>
- Alshatshati, S. F. (2017). *Estimating Envelope Thermal Characteristics From Single Point in Time Thermal Images* (University of Dayton). Retrieved from <https://pdfs.semanticscholar.org/ee4b/4c1803850f5fa07edc183ad9ed7f27f88e02.pdf>
- Antonopoulos, K. A., & Koronaki, E. (1998). Apparent and effective thermal capacitance of buildings. *Energy*. [https://doi.org/10.1016/S0360-5442\(97\)00088-1](https://doi.org/10.1016/S0360-5442(97)00088-1)
- Architecture 2030. (2018). Architecture 2030 - Existing Buildings. Retrieved September 9, 2019, from <https://architecture2030.org/existing-buildings-operation/>
- ASTM. (2013a). *ASTM C1046: Standard Practice for In-Situ Measurement of Heat Flux and Temperature on Building Envelope Components*. Retrieved from <https://www.astm.org/Standards/C1046.htm>
- ASTM. (2013b). *ASTM C1155: Standard Practice for Determining Thermal Resistance of Building Envelope Components from the In-Situ Data*. Retrieved from <https://www.astm.org/Standards/C1155.htm>
- Balaras, C. A., & Argiriou, A. A. (2002). Infrared thermography for building diagnostics. *Energy and Buildings*. [https://doi.org/10.1016/S0378-7788\(01\)00105-0](https://doi.org/10.1016/S0378-7788(01)00105-0)
- Braun, J. E., & Chaturvedi, N. (2002). An inverse gray-box model for transient building load prediction. *HVAC&R Research*, 8(1), 73–99.
- Chen, Y., & Chen, Z. (2000). A neural-network-based experimental technique for determining z-transfer function coefficients of a building envelope. *Building and Environment*, 35(3), 181–189. [https://doi.org/10.1016/S0360-1323\(99\)00010-4](https://doi.org/10.1016/S0360-1323(99)00010-4)
- Cho, Y., Bianchi-Berthouze, N., Marquardt, N., & Julier, S. J. (2018). Deep thermal imaging: proximate material type recognition in the wild through deep learning of spatial surface temperature patterns. *Proceedings of the 2018 CHI Conference on Human Factors in Computing Systems*, 1–13.
- Deru, M., Field, K., Studer, D., Benne, K., Griffith, B., Torcellini, P., ... others. (2011). *US Department of Energy commercial reference building models of the national building stock*. Retrieved from National Renewable Energy Laboratory website: https://digitalscholarship.unlv.edu/cgi/viewcontent.cgi?article=1045&context=renew_pubs
- DOE. (2012). Energy Department Announces Six Projects to Develop Energy-Saving Windows, Roofs, and Heating and Cooling Equipment. Retrieved September 9, 2019, from <https://www.energy.gov/articles/energy-department-announces-six-projects-develop-energy-saving-windows-roofs-and-heating>
- DOE. (2020). EnergyPlus Weather Data. Retrieved December 7, 2019, from <https://energyplus.net/weather>
- EIA. (2012). *2012 Commercial Buildings Energy Consumption Survey (CBECS)*. Retrieved from <https://www.eia.gov/consumption/commercial/data/2012/bc/pdf/b1-b46.pdf>
- Grossmann, C., Roos, H.-G., & Stynes, M. (n.d.). *Numerical Treatment of Partial Differential Equations*. Springer Science & Business Media.
- Haberl, J. S., & Bou-Saada, T. E. (1998). Procedures for Calibrating Hourly Simulation Models to Measured Building Energy and Environmental Data. *Journal of Solar Energy Engineering*, 120(3), 193–204. <https://doi.org/10.1115/1.2888069>
- Heo, Y., Choudhary, R., & Augenbroe, G. A. (2012). Calibration of building energy models for retrofit analysis under uncertainty. *Energy and Buildings*. <https://doi.org/10.1016/j.enbuild.2011.12.029>
- IEA. (2019). IEA Energy Efficiency: Buildings. Retrieved September 9, 2019, from <https://www.iea.org/topics/energyefficiency/buildings/>
- Jiménez, M. J., Madsen, H., & Andersen, K. K. (2008). Identification of the main thermal characteristics of building components using MATLAB. *Building and Environment*, 43(2), 170–180. <https://doi.org/10.1016/j.buildenv.2006.10.030>
- Kramer, R. P., & van Schijndel, A. W. M. (2012). Inverse modeling of climate responses of monumental buildings. *ArXiv Preprint ArXiv:1206.4438*.
- Kramer, R., van Schijndel, J., & Schellen, H. (2012). Simplified thermal and hygric building models: A

- literature review. *Frontiers of Architectural Research*.
<https://doi.org/10.1016/j.foar.2012.09.001>
- Krutz, G. W., Schoenhals, R. J., & Horc, P. S. (1978). Application of the Finite-Element Method to the Inverse Heat Conduction Problem. *Numerical Heat Transfer*, 1(4), 489–498.
<https://doi.org/10.1080/10407797809412181>
- Norlén, U. (1990). Estimating thermal parameters of outdoor test cells. *Building and Environment*.
[https://doi.org/10.1016/0360-1323\(90\)90036-Q](https://doi.org/10.1016/0360-1323(90)90036-Q)
- Rakha, T., & Gorodetsky, A. (2018, September 1). Review of Unmanned Aerial System (UAS) applications in the built environment: Towards automated building inspection procedures using drones. *Automation in Construction*, Vol. 93, pp. 252–264.
<https://doi.org/10.1016/j.autcon.2018.05.002>
- Ramallo-González, A. P. (2013). *Modelling, simulation and optimisation of low-energy buildings*.
- Reinhart, C. F., & Cerezo Davila, C. (2016). Urban building energy modeling - A review of a nascent field. *Building and Environment*.
<https://doi.org/10.1016/j.buildenv.2015.12.001>
- Tseng, A. A., Chen, T. C., & Zhao, F. Z. (1995). DIRECT SENSITIVITY COEFFICIENT METHOD FOR SOLVING TWO-DIMENSIONAL INVERSE HEAT CONDUCTION PROBLEMS BY FINITE-ELEMENT SCHEME. *Numerical Heat Transfer, Part B: Fundamentals*, 27(3), 291–307.
<https://doi.org/10.1080/10407799508914958>
- Vallerand, S., & Maldague, X. (2000). Defect characterization in pulsed thermography: a statistical method compared with Kohonen and Perceptron neural networks. *NDT & E International*, 33(5), 307–315.
- van Schijndel, A. W. M. (2009). The Exploration of an Inverse Problem Technique to Obtain Material Properties of a Building Construction. In *4th International Building Physics Conference*.
- Wang, S., & Xu, X. (2006). Parameter estimation of internal thermal mass of building dynamic models using genetic algorithm. *Energy Conversion and Management*.
<https://doi.org/10.1016/j.enconman.2005.09.011>
- Xu, X., & Wang, S. (2008). A simplified dynamic model for existing buildings using CTF and thermal network models. *International Journal of Thermal Sciences*.
<https://doi.org/10.1016/j.ijthermalsci.2007.10.011>
- Zhang, Y., O'Neill, Z., Dong, B., & Augenbroe, G. (2015). Comparisons of inverse modeling approaches for predicting building energy performance. *Building and Environment*.
<https://doi.org/10.1016/j.buildenv.2014.12.023>